Temporary stratification promotes large greenhouse gas emissions in a shallow eutrophic lake

Thomas A Davidson[1, 2], Martin Søndergaard[1, 2, 3], Joachim Audet[1, 2], Eti Levi[1], Chiara Esposito[1, 2], Tuba Bucak Onay[1], Anders Nielsen[1,4].

[1] Lake Ecology, Department of Ecoscience, Aarhus University, Denmark

[2] WATEC Aarhus University Centre for Water Technology, Aarhus University, Denmark

[3.] Sino-Danish Centre for Education and Research (SDC), Beijing, China

[4.] WaterITech Aps, Døjsøvej 1, 8660 Skanderborg, Denmark

Corresponding author: Thomas A Davidson, Department of Ecoscience, Aarhus University, C. F. Møllers Alle 4-6, DK-8000 Aarhus C, Denmark, e-mail: thd@ecos.au.dk

Abstract

Shallow lakes and ponds undergo frequent temporary thermal stratification. How this affects greenhouse gas (GHG) emissions is moot, with both increased and reduced GHG emissions hypothesised. Here, weekly estimation of GHG emissions, over growing season from May to September, were combined with temperature and oxygen profiles of an 11 hectare temperate shallow lake to investigate how thermal stratification shapes GHG emissions. There were three main stratification periods with profound anoxia occurring in the bottom waters upon isolation from the atmosphere. Average diffusive emissions of methane (CH_4) and nitrous oxide (N_2O) were larger and more variable in the stratified phase, whereas carbon dioxide (CO_2) was on average lower, though these differences were not statistically significant. In contrast, there was a significant, order of magnitude, increase in CH_4 ebullition in the stratified phase. Furthermore, at the end of the period of stratification, there was a large efflux of CH_4 and CO_2 as the lake mixed. Two relatively isolated turnover events were estimated to have released the majority of the CH_4 emitted between May and September. These results demonstrate how stratification patterns can shape GHG emissions and highlight the role of turnover emissions and the need for high frequency measurements of GHG emission which are required to accurately characterise emissions, particularly from temporarily stratifying lakes.

Keywords: Climate change; lake stratification; methane; carbon dioxide; nitrous oxide; climate feedbacks

1. Introduction

Fresh waters are key sites for the processing of greenhouse gases (GHG), methane (CH_4), carbon dioxide (CO_2) and nitrous oxide (N_2O). Shallow lakes, in particular, have been identified as hot spots of CH_4 release, particularly when ebullition is taken into account (Davidson et al., 2018; Aben et al., 2017). The certainty that fresh waters are large emitters of GHGs contrasts with the uncertainties associated with the quantities emitted and this is in large part due to historical paucity of measurements (Cole, 2013). A recent study identified the highly variable emissions from lakes and ponds which contribute to more than half the total emissions (Rosentreter et al., 2021). Whilst different morphometric features and chlorophyll-a explained some of the emission patterns (Deemer and Holgerson, 2021), it is also clear that a dearth of measurement combined with these highly variable emissions makes determining the drivers and controls of those emissions a challenge, which in turn makes predicting future emissions difficult.

The current and future effects of climate change on lakes in general and on their GHG emissions are relevant questions as there is potential for positive feedbacks and synergies with other human impacts such as eutrophication (Davidson et al., 2018; Beaulieu et al., 2019; Delsontro et al., 2016; Meerhoff et al., 2022). Taking a broad metabolic theory of ecology approach, temperature increases should promote methanogenesis and shift the balance from primary production to respiration increasing CO_2 emission at cellular and ecosystem scale (Yvon-Durocher et al., 2010). However, empirical and experimental data indicate that temperature is not the sole control of primary production and methanogenesis. In particular, eutrophication, and the promotion of large algal crop, has been associated with increased emissions of CH_4 and N_2O (Delsontro et al., 2016) both by diffusion and ebullition (Zhou et al., 2019). Furthermore, in what is globally the most abundant lake type, small shallow lakes, where macrophytes can colonise large areas of the lake bed, trophic state and the dominance of submerged plants or algae may be more important than temperature in shaping GHG dynamics (Davidson et al., 2015; Davidson et al., 2018; Bastviken et al., 2023).

Climate change effects on lakes are not limited to increases in average temperatures and lengthening of the growing season. Increases in both the frequency and intensity of heat waves are predicted, which will promote the warming of surface waters and in turn make permanent and temporary thermal stratification of lakes more likely (Woolway and Merchant, 2019), even in lakes typically classified as non-stratifying (Kirillin and Shatwell, 2016). A recent study Holgerson et al. (2022) identified stratification and mixing patterns in small water bodies, with permanent summer stratification common and frequent mixing occurring in larger standing waters (>4 ha) lakes. Such periods of stratification and mixing events are likely to have profound effects on GHG dynamics. Emissions of gases, in particular CH_4, that accumulate in the isolated bottom waters of a stratified lake, occurs upon mixing and can make very significant contributions to cumulative emissions (Schubert et al., 2012). High-resolution studies of sites that undergo temporary stratification are, however, rare (Søndergaard et al., 2023). In terms of its effects on GHG dynamics, there are potentially antagonistic processes at work in a stratified lake. On the one hand the 'shield effect' results in lower temperatures at the sediment surface slowing down metabolic processes that scale with temperature, i.e. methanogenesis and mineralization of organic carbon (C), reducing emission and promoting C burial. On the other hand, anoxia at the sediment surface may shift processes towards fermentation, increasing the proportion and total amount of CH_4 produced and perhaps reducing C burial (Bartosiewicz et al., 2019). Recent work combining empirical observations and models has suggested that shielding effects are larger than the anoxia effects and that stratification, in general, increases C burial and reduces GHG emissions (Bartosiewicz et al., 2015). The stratification induced isolation of bottom waters was reported to lead to reduced ebullition of CH_4 and a shift to diffusive pathways. It might, however, be predicted that in shallow lakes stratification would lead to much larger CH_4 release as anoxic conditions would limit CH_4 oxidation by CH_4 oxidizing bacteria (MOBs) (Bastviken et al., 2008). There may also be other factors with the potential to increase GHG emission, such as sediment organic content and lake trophic status (Delsontro et al., 2016), which may interact with stratification patterns in shaping GHG emissions.

In this study, we used data from a shallow lake with high frequency measurements of temperature profiles combined with weekly measurements of dissolved gas concentrations in the surface and bottom waters and continuous measurement of ebullitive emissions of CH_4 to track the effects of lake stratification on GHG emissions. The key question was how ebullitive and diffusive fluxes of the key GHGs: CH_4, CO_2 and N_2O respond to temporary thermal stratification.

2. Materials and methods.

2.1 Study site

Ormstrup lake, located in Denmark (lat 56.326°, lon 9.639°) (Fig.1) (depth map with GHG sampling locations), is an 11 ha, shallow lake (average depth 3.4 m), with a maximum depth of 5.5 m, and with a relatively long hydraulic retention time (> 1 year). The lake is eutrophic with high TP and chlorophyll-a (Table 1; Søndergaard et al., 2022) with very sparse occurrence of submerged plants.

2.2 Depth profiling and high frequency measurements

In June 2020, a Nexsens (NexSens Technology, Fairborn, OH, USA) CB-450 data buoy system (https://www.nexsens.com/pdf/CB450_datasheet.pdf) was deployed at the deepest point of the lake equipped with a Nexsens TS210 thermistor string https://www.nexsens.com/pdf/TS210_datasheet.pdf) with temperature nodes measuring at 4 levels; one sensor “in air”, ca. 5 cm above the water surface, (but shielded from direct light), and three sensors at -1, -2, -3 meters, respectively relative to the water surface. In addition two Aqua TROLL 500 (In-Situ, Fort Collins, CO, USA) multi-sondes were mounted near the surface (-1.0 meters) and at deeper water depth (-3.8 meters). The near surface and deeper water sonde were configured with sensors to measure dissolved oxygen (DO) and water temperature (Tw). The optical sensors were calibrated according to manufacture guidelines and checked on a weekly basis.

The optical sensors of the Aqua TROLL 500 have a built-in wiper mechanism to clean sensor heads to hamper bio-fouling. The wiper function was enabled to perform cleaning in sync with sensor measurements, hence every 15 minutes. In addition, manual cleaning of sensor heads was done every week, while routine manual field monitoring was carried out at the lake. Prior to the deployment of the buoy, and as a validation exercise for the buoy data, weekly manual profiles of DO and Tw were collected at the deepest point.

Periods of stratification were defined by a greater than 2 °C difference between the surface and bottom waters and DO below 0.5 mg l^{-1} at the time of the weekly manual profiling of the system. The high frequency measurements were used to confirm the patterns. During periods of defined as stratified, there were partial mixing events where the depth of the thermocline and oxycline change and there was some mixing of the bottom waters and surface waters. of the water column mixes, whilst the bottom waters remained undisturbed as the DO did not increase the partial mixing above might increase gas exchange.

2.3 Water chemistry

Water samples for the analysis of Chlorophyll-a were collected weekly from the 20. April 2020 from surface (-0.5 m) water at station 3 (Fig. (Søndergaard et al., 2005)1). A volume of water ranging from (0.2 to 1 litre) was filtered and the GFC papers preserved for chlorophyll-a analysis, which were determined spectrophotometrically after ethanol extraction (Jespersen and Christoffersen, 1987) and alkalinity was measured weekly by gran titration (Søndergaard et al., 2005). Depth profiles of temperature, electrical conductivity (EC) and dissolved oxygen (DO) were measured manually with an Aqua TROLL 500 probe from every -0.5 or -1 m down to -5 m depth).

2.4 Greenhouse gas sampling

2.4.1 Dissolved concentration

Samples of dissolved concentrations of CH_4, CO_2 and N_2O were collected weekly from the 20. April 2020 from surface waters and weekly from surface and bottom water from the 26. May 2020. The samples were taken using head-space equilibration after (Mcauliffe, 1971), where 20 ml of water was collected from just below the water surface and 20 ml of N_2 was introduced as a headspace in a 60-ml syringe and then shaken vigorously for one minute. The 20 ml headspace was then transferred to a 12-ml pre evacuated glass vial.

Gas concentrations in the headspace were determined on a dual-inlet Agilent 7890 GC system interfaced with a CTC CombiPal autosampler (Agilent, Nærum, Denmark) (Petersen et al., 2012). For the GC, certified CO_2, CH_4 and N_2O standards were used for calibration and validation. Aqueous concentrations in N_2O, CH_4 and CO_2 were calculated from the headspace gas concentrations according to Henry's law and using Henry's constant corrected for temperature and salinity (Weiss, 1974; Weiss and Price, 1980; Wiesenburg and Guinasso, 1979). A recent study (Koschorreck et al., 2021) identified significant bias in the estimate of CO_2 concentrations using headspace equilibration at lower concentrations. We applied their correction using separately measured alkalinity as described in Koschorreck et al. (2021).

The fluxes of N_2O, CH_4 and CO_2 between the water and the overlying atmosphere were estimated as

$$f_g = k_g\left(C_{wat,g} - C_{eq,g}\right)$$

Where f_g is the flux of a specific gas g, k_g is the piston velocity of the gas and $C_{wat,g} - C_{eq,g}$ is the gradient of concentration between the concentration of gas dissolved in the water ($C_{wat,g}$) and the concentration of gas the water would have at equilibrium with the atmosphere ($C_{eq,g}$).

We calculated a gas transfer velocity k_{600} for each sampling occasion using the relationship based on windspeed described in (Cole and Caraco, 1998).

$$k_{600} = 2.07 + 0.215U_{10}^{1.7}$$

161 U_{10} is the mean daily windspeed at 10m (m s^{-1}) obtained from the Danish meteorological institute
162 (DMI;20x20 km grid data)
163
164
165 $$k_g = k_{600}\left(\frac{Sc_g}{600}\right)^x$$
166
167 Sc_g is the Schmidt number(Wanninkhof, 1992) of the specific gas g. We chose x =-2/3 as this factor is
168 used for smooth liquid surface (Deacon, 1981).
169
170 Daily flux rates were calculated using linear interpolation of the weekly surface measurements from each
171 of the sampling points. The diffusive surface water fluxes were calculated by taking an average of the daily
172 flux rate from the 12. May 2020 to the 13. October 2020 for each location. Then an average of the 3 locations
173 was multiplied by the area of the lake and the number of days covered by the study, here 126 days was
174 chosen to match the period over which ebullition was measured.
175
176 The total content of the gases in the lake's bottom waters were calculated from the concentration of the
177 gases per litre multiplied by an estimate of the volume of the water in the hypolimnion. The volume of
178 water in the hypolimnion was estimated from the lake profiles manually conducted on the day of
179 sampling. The top of the hypolimnion was determined by the depth below which oxygen was less than 0.5
180 mg l^{-1}. A detailed bathymetry of the lake allows the calculation of the area and therefore volume of water
181 that lies below a given depth.
182
183 During the study period two major turnover events occurred, the process of lake turnover and full mixing
184 can take a number of days, and the outgassing even longer. The oxygen data, from the buoy, indicated
185 that it can take up to four days and this provides time for CH_4 oxidation to occur (Søndergaard et al.,

2023). In order to estimate the amount of CH_4 oxidised over the course of the multiple days of degassing we directly measured CH_4 oxidation rates in the surface waters of the lake. This was done in June 2023 in five locations using methods outlined in (Thottathil et al., 2019) where five water samples from five different locations and each was incubated over 4 days with and the change in CH_4 concentration used to calculate oxidation rates. We used the minimum (0.267 µg CH_4-C l^{-1} h^{-1}), mean (0.44 µg CH_4-C l^{-1} h^{-1}) and maximum (0.58 µg CH_4-C l^{-1} h^{-1}) oxidation rates to estimate the range of CH_4 oxidation likely to have occurred over the course of the two main turnover events. Assuming that the degassing took four days, these rates would consume between 2 and 8% of the CH_4 contained in the hypolimnion. Using the mean oxidation value the turnover fluxes were reduced by 4.1% on the 30th of June 2020 and by 6% for the 25th August 2022.

2.4.2 Ebullition

The ebullitive flux of CH_4 was estimated using at total of 40 floating chambers placed on 4 transects of 10 chambers each (Fig. 1). The chambers have a volume of 8 litre and a surface area of 0.075 m^2, similar to those used by (Bastviken et al., 2015). As the existing literature indicated that ebullition is lower as water depth increases (Wik et al., 2013) the transects were placed to maximise the measurement of the low end of the depth gradient on the shallower slopes of the western end of the lake (Fig. 1). The average and maximum depth of each transect was T1: 293 cm and 472 cm; T2: 181 cm and 267, T3: 223 cm and 300 cm and T4 166 cm and 220 cm.The chambers were set on the 14. May 2020 and sampled every two weeks from that date, and on one occasion after one week until September 17th, which is a period of 127 days. Twenty ml of sample was taken from the floating chamber and injected into a pre-evacuated 12 ml vial (exetainer, Labco). Gas concentrations were determined on the same GC than described above (Petersen et al., 2012)

Ebullitive flux of CH_4 was estimated as:

$$\frac{p_{gas} \times Vol_{bub}}{t \times A}$$

Where p_{gas} is the concentration of CH_4 in the gas that was trapped, Vol_{bub} is the volume of the chamber (i.e. 7L), t is the time during which the samples was collected and A is the area of chamber (i.e. 0.075 m^2). A portion of the CH_4 released via ebullition in the chamber will have re-dissolved in the water or might leak through the chamber walls, thus underestimating the ebullitive flux. We have made a number of measurements to constrain this error and to compare estimates based on static chambers with other approaches. The result show that whilst static chambers underestimate ebullition, given the temporal variability of ebullition, static chambers continually deployed provide a better estimate of average ebullition than short term (24-48 hours) deployment using portable gas monitors or flushing chambers.

Therefore, whilst static chambers method cannot be said to accurately quantify CH_4 emissions, they can be relied upon to compare differences in ebullition between time periods, with the caveat that they are always an underestimate of actual ebullitive flux.

Total ebullitive flux from the lake was calculated by taking a mean of the emissions from each transect over the 126 day period. Then taking an average of the means of four transects and multiplying this by the time of deployment of the chambers in days, which was 126 days, and by the area of the lake. This gives a total ebullitive flux of CH_4 for the lake over the period of measurement from May to mid September.

The three different flux types, surface diffusion, ebullition and turnover emission were then converted in comparable units of total lakes emissions (as g or kg of gas) over the studied period and also converted into CO_2-equivalents using a conversion factor related to their 100 year global warming potential (GWP) of 28 for CH_4 and 265 for N_2O.

2.5 Statistical methods

To test for a significant difference among the emissions from the stratified and mixed phase we used generalised least squares (GLS) with a variance function to account for heterogeneity of variance between the phases. In the case of the ebullitive flux, as the collected phase often covered periods including both mixed and stratified phases there were three categories, mixed, stratified and both mixed and stratified. All analysis was carried out in R version 4.2.1 (R Development Core Team, 2022) and the GLS used the package nlme (Pinheiro et al., 2014).

3.0 Results

3.1 Lake physical and chemical characteristics

Depth profiles measured weekly from April show that stratification was initiated by the 26. May 2020 this may have broken down briefly and established again, visible in the temperature sensors for the buoy on the 5. June 2020 (Fig. 2). There were then 12 days of mixing followed by stable period of stratification with onset the 14. June 2020 and a duration of 16 days until a mixing event around the 30. June 2020. The following two weeks had cooler water and a mixed water column, herafter a ca. 6 day period of stratification from the 15. to 21. July 2020. A mixed phase of two weeks then followed until stratification reestablished on 4. August 2020 and persisted until the end of August, partial mixing is indicated by the buoy data from the 21. August 2020, but the weekly manual profile to deeper water inidcate that full mixing did not occur until after the 25. August 2020. The effects of the stratification and mixing events on the high frequency DO data measured at -3.8 m are clear, with rapid deoxygenation occuring after the onset of stratification and oxic bottom waters returning when the lake mixed (Fig, 2). The pattern in chlorophyll-a also follow, to some degree, those of stratification, with the exception of early spring. Chlorophyll-a values were extremely high in spring peaking at the start of June 2020 and falling gradually (Fig. 2). (Søndergaard et al., 2023)During the periods of stratification chlorophyll biomass was lower, and

257 when a mixing event occurred the values increased, which is particularly evident in the July mixing
258 periods (Fig. 2).
259
260 **3.2 Concentrations of dissolved gases and fluxes from the surface waters.**
261 The concentrations of the dissolved gases showed great variation from near or below atmospheric
262 concentrations in some cases and up to an extremely high concentration (over 5 mg CH_4 C l^{-1}) in the
263 bottom waters on the 30. June 2020. There was some spatial heterogeneity in the surface waters, with the
264 more littoral locations showing the greatest variation and the highest values (Figs. 3,4,5). In particular the
265 most littoral zone, where the water was shallower around 1 m in depth, showed the highest values just
266 prior to, or coincident with, the stratification turnover. Table 2 shows the mean diffusive flux of each gas
267 over the sampling period along with the mean flux in mixed and stratified phases. For CO_2 there was a lot
268 of temporal variation in flux dynamics, though not a large difference between mixed and stratified phases
269 in terms of mean values (Table 2). There were some periods of CO_2 influx in spring and later summer and
270 these tended to coincide with the end of a mixed phase and the start of the stratification phase. Nitrous
271 oxide concentrations were generally low (Figs 4 & 5) with the lake being a source of N_2O in the spring
272 period and a sink or a very small source thereafter. The CH_4 concentration in the surface waters (Fig. 3)
273 and the calculated diffusive emissions are relatively low, but did increase in the stratification periods with
274 higher average values (Table 2 & Fig. 6). There was also some spatial variation with higher CO_2 and CH_4
275 diffusive emissions in the shallower sampling locations, both in stratified and mixed conditions (Fig. 6).
276
277 The most marked patterns in GHG concentration were evident in the bottom waters sampled at -4.5 m,
278 which accumulated to very large concentrations of CO_2 but particularly CH_4 in the periods of
279 stratification (Fig. 3 & 4). The ratio of CO_2 to CH_4 is illustrative in highlighting how stratification has
280 altered the biogeochemical processes in the hypolimnion with CH_4 production becoming more prevalent. .

For example on 30. June 2020 after 16 days of stratification the the ratio CO_2:CH_4 in the bottom waters was 0.8, whereas 7 days later after the mixing event it was 187 at the same depth.

3.3 Ebullitive fluxes

The CH_4 bubble flux, presented here as mean values for each of the 4 transects, ranged from 0.303 to 81.1 mg CH_4 C m^2 d^{-1} for the individual transect over the growing season measurement. There is a very clear, statistically significant impact of stratification on the ebulltive efflux of CH_4 with stratified periods showing significantly markedly higher levels of emission (Fig. 7 and Table 2). In addition, there was a difference in average emissions among the different transects, with those with lower average water depth (T2 & T4) having lower emission than the transects with chambers over deeper water (T1 & T3) (Fig. 7). The samples collected from the chambers reflect two weeks of bubble and diffusion collection and the quantification of the flux is therefore an average of the period of chamber deployment, which was two weeks, or in one case a single week (Fig. 7). This two week period on occasion covered both stratified and mixed phases and on these occassions efflux was intermediate between purely mixed and stratified periods (Table 2 and Fig. 7).

3.4 Total lake fluxes

Scaling up the results to total flux of gases from the whole lake over the period of study and including the estimated emissions from two turnover events show a very different effect of stratification on the balance of types of emissions for the three gases. The majority of CH_4 emission (56%) result from the two short-lived turnover events (Fig. 8), whereas their contribution to CO_2 and N_2O emission was 5% and 1% respectively.

Fluxes of CO_2 and N_2O were mostly diffusive, which represtented 95% of emissions of both gases. Methane diffusive flux was 14% of total emission, whereas CH_4 ebulltion was more than twice as much at

306 29% of total CH_4 emission. In terms of global warming potential CO_2 and CH_4 emission were
307 comparable, but the contribution of the turnover efflux was the dominant factor for CH_4 emissions.
308

309 # 4. Discussion

310 The emission of the three GHGs showed different degrees of variation between the mixed and stratified
311 phases. The largest and most significant variation was in CH_4 ebullition (Table 2), whilst the difference in
312 diffusive fluxes, though marked for CH_4 was not significant. The mean of the total emissions from
313 Ormstrup in the stratified phase (59.9 mg CH_4-C m^{-2} day^{-1}) corresponds relatively closely to the mean of
314 the total emissions (ebullition plus diffusion) reported for lakes in this size range (47 mg CH_4-C m^{-2} day^{-1})
315 from a paper synthesising multiple studies (Rosentreter et al., 2021). The mean emissions for the whole
316 period (26.6 CH_4 -C m^{-2} day^{-1}) were lower than Rosentreter et al. (2021) but similar to other studies with
317 mean emissions of 30.9, 20.7 and 22.7 CH_4 -C m^{-2} day^{-1} and were reported by Peacock et al. (2021), Sø et
318 al. (2023) and Peacock et al. (2019) respectively. Whereas the average CO_2 (504 mg CO_2-C m^{-2} day) at
319 Ormstrup was lower than 993.5 1 mg CO_2-C m^{-2} day^{-1} measured by Peacock et al. (2021) but higher than
320 the 264.6 and 205.1 mg CO_2-C m^{-2} day^{-1} measured by Sø et al. (2023) and Peacock et al. (2019)
321 respectively. The different temporal resolution and duration of these studies, eleven single day sampling
322 from April to December (Peacock et al., 2021), five days continuous sampling on one occasion in late
323 September (Sø et al., 2023) and a single early summer snapshot (Peacock et al., 2019) make direct
324 comparison difficult. The data here do, however, provide a clear answer to the question of how thermal
325 stratification effects GHG dynamics in shallow eutrophic lakes with an increase in total emissions
326 (diffusion, ebullition and turnover) during the stratified period (Table 2, Fig 9). Previous work, combining
327 observations and modelling suggested the opposite patterns (Bartosiewicz et al., 2019) as the shielding
328 effect of the stratification results in cooler bottom waters which reduces CH_4 production due to the
329 process being temperature dependent (Bartosiewicz et al., 2016). This strong shielding effect may apply
330 in deeper lakes experiencing more stable stratification, or less eutrophic lakes. The result here from a

relatively shallow eutrophic lake, indicate that temporary stratification causes increases in GHG emissions.

Diffusive emissions did not, on average, show a strong stratification effect (Table 2). In particular variation in N_2O emissions did not match patterns of stratification, with emissions more directly related to nitrate concentrations (Audet et al., 2020), as reflected by the fact the lake is a sink of N_2O in late summer when nitrate was below detection limits for several weeks. There were peaks in emission of CH_4 and CO_2 at the end of stratification periods, particularly in the shallower water sampling points (Fig. 6). There were periods of influx of CO_2, which coincided somewhat with periods of stratification, but the patterb was not consistent as other factors, for example, chlorophyll-a concentration also play a role.

Littoral zones can have markedly different GHG dynamics to deeper zones due to shallower water having lower pressure (Wik et al., 2013), less time for CH_4 oxidation (Bastviken et al., 2008) or abundant plants which influence a range of biogeochemical processes (Davidson et al., 2018; Esposito et al., 2023). It is therefore possible that littoral zone dynamics could cause these differences. However, the increase occurred at all three sampling points at the end of June 2020, which indicates a lake-wide driver and the peak may represent the start of mixing after stratification. Strong winds were measured on the 29th and 30th June 2020 (Søndergaard et al., 2023) coincident with these increased littoral emissions. These winds would have caused lateral movement of the surface water causing an upwelling of bottom water, rich in CH_4 and CO_2, in the littoral margins at the opposite end of the lake. Thus, whilst we do not have direct evidence it seems more likely that these increased emissions in the littoral zone were driven, at least in part, by the upwelling of GHG rich bottom waters.

In contrast to the diffusive flux, the ebullitive emission of CH_4 shows a very clear response to stratification with an order of magnitude difference in emissions between periods where the sampling reflected purely mixed or stratified periods (Table 2 & Fig. 7). The two-week resolution of the sampling

meant that some samples covered both stratified and mixed phases and these samples had intermediate fluxes, as they cover both low (mixed) and high emission (stratified) periods. The spatial variation in ebullition is also illustrative of the impacts of stratification and the role of anoxia in shaping CH_4 fluxes. The two transects with the largest mean and maximum depths (T1 and T3) had the largest emissions, with the deeper of the two (T1) having the highest emissions and they saw the greatest relative increase during the stratification phases. This pattern is different to that found in other studies where bubble emissions were larger in shallower water, although later in the summer there was in increase in bubble flux (Wik et al., 2013). The deeper water at Ormstrup experienced anoxia earlier and this appears to cause locations with deeper water to have higher ebullition rates than shallower areas. This is at odds with ideas stemming from the metabolic theory of ecology stating that temperature (Yvon-Durocher et al., 2014) in particular at the sediment surface (Bartosiewicz et al., 2019) can be used to predict CH_4 efflux. Whilst it is a fact that CH_4 production is temperature dependent at the cellular level, CH_4 emissions were rather independent of the sediment temperature, for example in the first two weeks of July 2020 emissions were low and the sediment surface temperature was relatively high. Thus, temperature alone is a poor predictor of ecosystem scale CH_4 emissions.

It should be noted that the methods used to estimate bubble flux here, where floating chambers are sampled every two weeks is a “less than perfect method”, which in nearly all cases will underestimate ebullitive flux. Logistical and financial constraints make continual sampling difficult and here we balanced these constrains against the greater time required to apply more accurate methods, such as bubble traps (Wik et al., 2013), automatic flushing chambers (Bastviken et al., 2015). Such is the variability of bubble flux in space and time that sampling campaigns covering days or weeks would potentially give an even more inaccurate picture of emissions than the method used here (see supplementary methods and supplementary materials). Though eddy covariance approaches offer a means of continuous measurement capable of capturing short term changes and covering a large area (Erkkilä et al., 2018).Thus, the continuous monitoring of ebullition using chambers with known biases was deemed

the least worst method available, but we acknowledge the caveat that ebullitive emissions may be underestimated.

In addition to the diffusive and ebullitive emissions, the turnover flux, which consists of the gases accumulated in the hypolimnion being released on turnover, was also estimated, with a correction of CH_4 oxidation applied. There were two major turnover events at the end of June and in late in August 2020, which were preceded by 16 and 22 days of stratification, respectively. It was not possible to directly-measure turnover flux, as they are relatively discrete events where the efflux likely occurs over the course of (Søndergaard et al., 2023)a few hours, or a few days. Thus, the efflux estimation is based on a series of assumptions and thus must be treated with caution. Notwithstanding this uncertainty, we can be confident the turnover flux represents a very large proportion of the total emission of CH_4 emissions from Ormstrup Lake over the growing season. We estimate it contributed more than 50 % of growing season CH_4 emissions and 5 % of CO_2 emissions. This highlights a very significant, and difficult to measure, contribution to GHG emissions from lakes undergoing temporary stratification, which are among the most common lake type in Denmark{Søndergaard, 2023 #8812} .

The results here suggest that GHG dynamics were driven both directly and indirectly by the stratification patterns and the anoxia it induced in the bottom waters. At Ormstrup Lake the thermal stratification of the water column quickly led to anoxia, with only a matter of hours to days for the oxygen to be consumed once the bottom waters were isolated (Fig. 2). The ratios of CO_2:CH_4 evidence how this promotes CH_4 over CO_2 production in the stratification phase (see Fig 9). In addition to promoting CH_4 production such conditions would preclude, or severely limit, oxic CH_4 oxidation, which has the potential to consume a large proportion of CH_4 produced in the anoxic sediments (Bastviken et al., 2008), though anoxic CH_4 can still occur (Blees et al., 2014). The raw emission data do not provide any direct information on the balance of production versus oxidation, but the CO_2:CH_4 suggest there was marked shift to conditions where methanogenesis was the dominant process and there was reduced CO_2 production. Studies have

409 shown that CH_4 oxidation can consume large proportions of the CH_4 produced under hypoxia (Saarela et
410 al., 2019) and it is possible that there is intense CH_4 oxidation occurring at the thermocline during the
411 periods of stratification at Ormstrup lake , but this was not directly measured at the lake. In addition to the
412 more direct effects of anoxia there may be some indirect effects of the patterns of stratification and
413 mixing that promote greater GHG emissions. Søndergaard et al. (2023) recently reported how nutrient
414 dynamics at Ormstrup Lake were altered by the lake stratification and full details can be found there, of
415 relevance here is the impact on chlorophyll-a which saw a large spring peak after which the abundance
416 tracked the stratification and mixing regime, with a lag time. There was a general reduction, or at least no
417 increase as the stratification period progressed, perhaps due to nutrient limitation in the epilimnion. Upon
418 mixing there was generally an increase in chlorophyll-a, though the weekly sampling resolution makes
419 this difficult to assess. Chlorophyll-a and the labile dissolved organic carbon (DOC) that result from
420 abundant chlorophyll-a have been shown to be associated with higher diffusive and ebullitive CH_4
421 emissions (Davidson et al., 2015; Beaulieu et al., 2019; West et al., 2012; Zhou et al., 2019). It is not
422 possible to say here whether a stable summer long stratification would have led to decreased chlorophyll-
423 a as nutrients became limiting due to their isolation in the bottom waters and reliable high frequency
424 chlorophyll-a data are required to convincingly demonstrate this phenomenon. Notwithstanding these
425 uncertainties it may be the case that the temporary stratification, interspersed with mixing events,
426 observed here represents a ‘sweet spot’ providing both the resources, i.e. chlorophyll-a and the labile
427 DOC it produces, and optimal conditions (anoxia) for CH_4 production.
428
429 Predicting climate change effects on GHG emissions in a future warmer world is not straightforward, as
430 there are multiple interacting drivers which combine to shape the GHG emissions of lakes. However, this
431 study suggests that temporary stratification, which is increasingly recognised as prevalent in ponds and
432 shallow lakes (Holgerson et al., 2022) and is likely to become more common with continued climate
433 change impacts (Woolway and Merchant, 2019) is likely to increase GHG emissions. This will be

particularly the case in more eutrophic systems where abundance algal derived dissolved organic matter can fuel CH_4 production (Zhou et al., 2019).

The combination of high frequency data on water temperature and dissolved oxygen combined with weekly measurements of GHGs increase the reliability of the findings presented here. Up until relatively recently it has been assumed that for shallow lakes, such as Ormstrup lake, stratification is not an important feature. Sampling has therefore focused on the surface layers of water bodies, using dissolved concentrations of gases or floating chambers to characterise flux, e.g. (Davidson et al., 2015; Audet et al., 2020; Peacock et al., 2021). Thus, most studies have overlooked bottom waters and do not have the temporal resolution required to capture turnover flux emissions from surface measurements. Furthermore, whilst many studies now include estimates of bubble emissions of CH_4 e.g. (Bergen et al., 2019), the necessary temporal resolution to accurately characterise ebullitive emission is not well established. The finding here indicated that in such dynamic systems near continuous measurement is desirable and that short term collection over one or two days could provide massive, over or under estimate of CH_4 ebullition.

Our results show very large temporal variation in emissions of all three gases, but in particular CO_2 and CH_4, and this highlights the need for high frequency measurements to accurately characterize emissions from lakes. Even the weekly frequency of the sampling in this study was not sufficient to directly measure all the emission pathways and turnover flux had to be inferred from bottom water calculations. These data show that to capture the extent of GHG emissions from lakes it is vital we include all forms of flux, including ebullition and turnover flux. Recent work has highlighted the fact that most emissions of CH_4 (over 50%) from fresh waters come from highly variable systems (Rosentreter et al., 2021), with the mean and median emission rates of CH_4 differing greatly, indicating a few large emitters are responsible for a large proportion of emissions. The sampling frequency applied here is rare, if a more standard resolution of monthly measurements was applied the emissions estimate of all the gases, but in particular CH_4,

would be highly dependent on what phase of the stratification was captured. As an example, a monthly sampling frequency could potentially miss all the stratification peaks - consequently massively underestimating emissions, whereas a different sampling frequency could catch a number of peaks and give a much higher estimate. Thus, the same sampling frequency on the same lake, but timed differently could lead to conclusions of highly variable emissions. Consequently, in these highly dynamic systems where temporary stratification occur in summer, high frequency measurements are required to accurately estimate emissions. This is logistically challenging but the current advances in the use of automatic flushing chambers (Bastviken et al., 2020) may provide the potential for affordable high spatial and temporal resolution measurement of GHG dynamics. This is a requisite for understanding the drivers of GHG dynamic, which is required for being able to predict how they will respond in a range of scenarios related to land use, climate change and management interventions.

Code/data availability

The datasets generated during and/or analysed during the current study are not publicly available as they form part of ongoing research projects but are available from the corresponding author on reasonable request and will be made publicly available later in the research project.

Author contributions

MS secured the funding for the wider lake restoration research project supplying the data. TAD, MS and JA conceptualized the gas study. TAD and AN established the buoy and sensor system. EL, CE, TAD, TB and JA collected and analysed the data. TAD wrote the paper and all authors commented on earlier versions and read and approved the final draft.

Competing interests

The authors declare that they have no conflicts of interest.

484

Acknowledgement

We thank our splendid technician team of Lene Vigh, Malene Kragh, Dorte Nedergaard and Dennis Hansen for their extreme competence on the lab and the field. We acknowledge Theis Kragh for the depth map of the lake already published in Søndergaard et al. 2023. We are very grateful to the Poul Due Jensen Foundation for providing great support for this work and the Ormstrup project generally. TAD and CE were also supported by GREENLAKES (No. 9040-00195B) and The European Union's Horizon 2020 research and innovation programmes under grant agreement No 869296—The PONDERFUL Project.

Table 1. Summary lake information, summer mean values and (standard deviation) of a range of variables

Variable	n	Year 2020
Secchi depth (m)	22	0.86 (0.28)
Chlorophyll a (µg/l)	20	53.4 (28.9)
pH	22	8.04 (0.77)
Total phosphorus (mg/l)	22	0.58 (0.11)
Total nitrogen (mg/l)	22	1.50 (0.41)

Table 2. Mean greenhouse gas flux (units CO_2: mg CO_2-C m^{-2} day^{-1}, N_2O: mg N_2O -N m^{-2} day^{-1}, CH_4 both diffusive and ebullitive in mg CH_4-C m^{-2} day^{-1}) from the lake from spring to Autumn 2020. The emissions are divided in diffusive, ebullitive emissions. The mean values for all the surface water stations and all four transects of chambers are given. Emissions area separated into mixed versus stratified phases and there SD are also given. Ebullition was collected for a period covering two weeks so on a number of occasion covered both mixed and stratified periods thus ebullition has a third category where both mixed and stratified conditions occurred is given. Ebullition was significantly different across the three phases, diffusive fluxes were not significantly different for *p* values of 0.05.

510

Emission type	gas	mean	mixed	Stratified	Strat and mixed
Diffusive	CO_2	493.7 (*529.6)*	559.6 *(433.1)*	449.8 *(587.6)*	
	CH_4	9.47 *(16.0)*	5.9 *(4.1)*	12.7 *(20.2)*	
	N_2O	0.11 *(0.09)*	0.09 *(0.08)*	0.12 *(0.11)*	
Ebullition	CH_4	17.28 *(19.62)*	**4.84** ***(3.44)***	**47.29** ***(21.95)***	**12.74** ***(10.34)***

511

512

513 Figure legends

514 Figure 1. Ormstrup lake bathymetry and sampling stations for surface water greenhouse gas sampling
515 (St1, St2, St3) bottom waters were sampled at S3. Transects of 10 bubble traps were placed on T1- T4.
516 Adapted from the Søndergaard et al. 2023.

517 Figure 2 Temperature profile from June 2020 when the buoy was deployed and surface and bottom water
518 oxygen from June to the end of September 2020. Manual chlorophyll-a (µg L^{-1}) values are also given in
519 the top panel.

520 Figure 3. Dissolved CH_4 concentrations from surface and bottom waters – thermal stratification periods
521 highlighted in grey and the white background indicate mixed waters

522 Figure 4 . Dissolved CO_2 concentrations from surface and bottom waters–thermal stratification periods
523 highlighted in grey and the white background indicate mixed waters

524 Figure 5 Dissolved N_2O gas concentrations surface and bottom thermal stratification periods highlighted
525 in grey and the white background indicate mixed waters

526 Figure 6. Omstrup lake surface fluxes of the CH_4, CO_2 and N_2O gases based on dissolved conentration ,
527 thermal stratification periods highlighted in grey and the white background indicate mixed waters

528 Figure 7. Plot of CH_4 ebullition averaged for each transect (10 chambers per transect), data collected from
529 40 traps every two weeks. Thermal stratification periods highlighted in grey and the white background
530 indicate mixed waters.

531 Figure 8 – Total lake emissions per gas over the growing season in CO_2 equivalents. The emissions are
532 divided different emission modes: Diffusive, ebullitive and turnover flux. All estimates constain some
533 uncertainty, in particular ebulltive flux is an underestimate and the turnover flux also contains a gret deal
534 of uncertainty.

Figure 9. Summary of the quantities of the gases present in the water and the volumes emited from the different pathways. The size of the arrow is proportional to the emissions from each pathway and with the startified state on the left and the mixed state on the right, with the turnover flux in the centre.

539 Figures and legends

540 Figure 1.

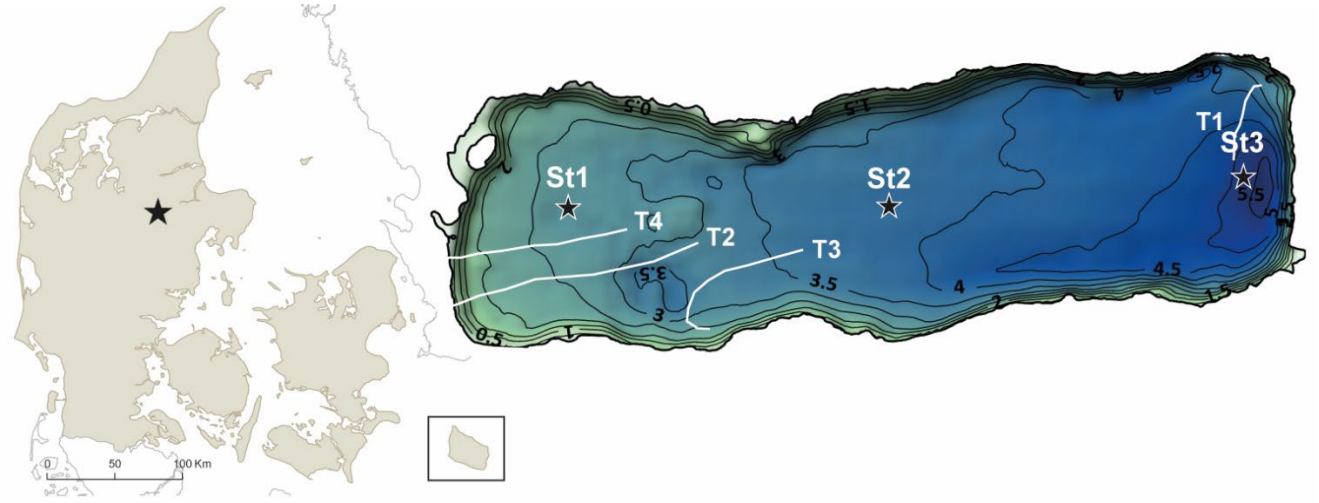

541

542 Figure 1. Ormstrup lake bathymetry and sampling stations for surface water greenhouse gas sampling (S1,
543 S2, S3) bottom waters were sampled at S3. Transects of 10 bubble traps were placed on T1- T4. Adapted
544 from the Søndergaard et al. 2023.

545

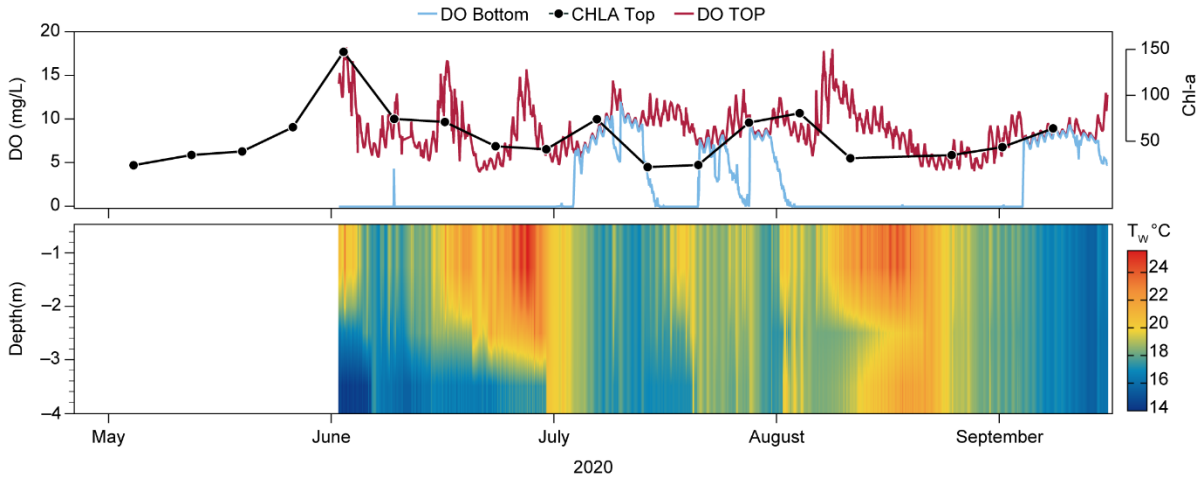

546

547 Figure 2 Temperature profile from June when the buoy was deployed and surface and bottom water
548 oxygen from June to the end of September. Chlorophyll-a (µg L^{-1}) values are also given in the top panel
549 and surface (DO TOP) and bottom (DO Bottom) dissolved oxygen (mg L^{-1}) are also given

550

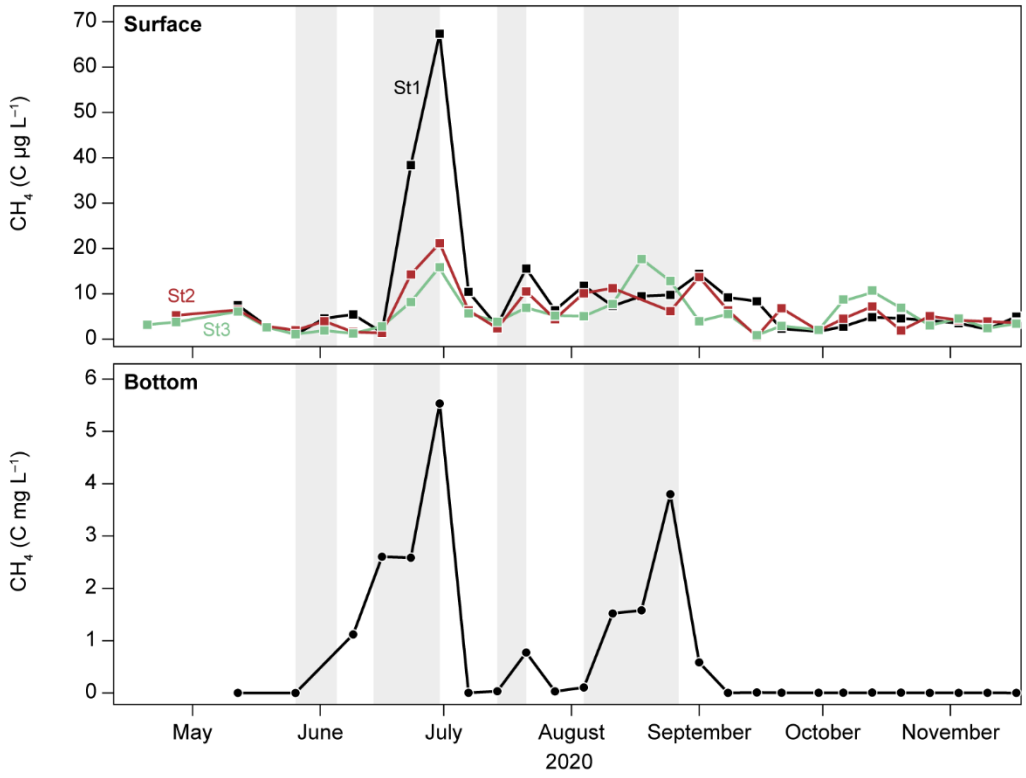

551

552 Figure 3. Dissolved CH_4 concentrations from surface and bottom waters – thermal stratification periods
553 highlighted in grey; white background indicate mixed waters. Note different y axis scales

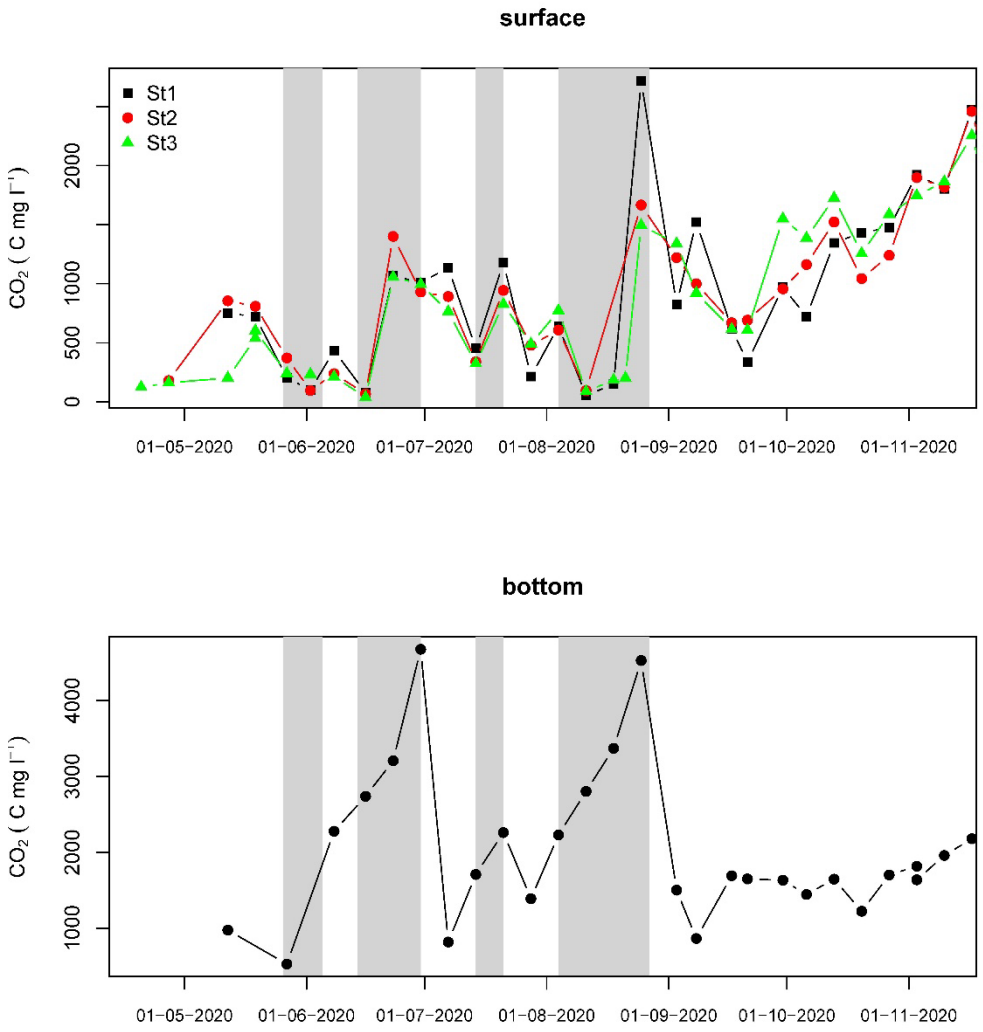

554

555 Figure 4 . Dissolved CO_2 concentrations from surface and bottom waters–

556 thermal stratification periods highlighted in grey; white background indicate mixed waters

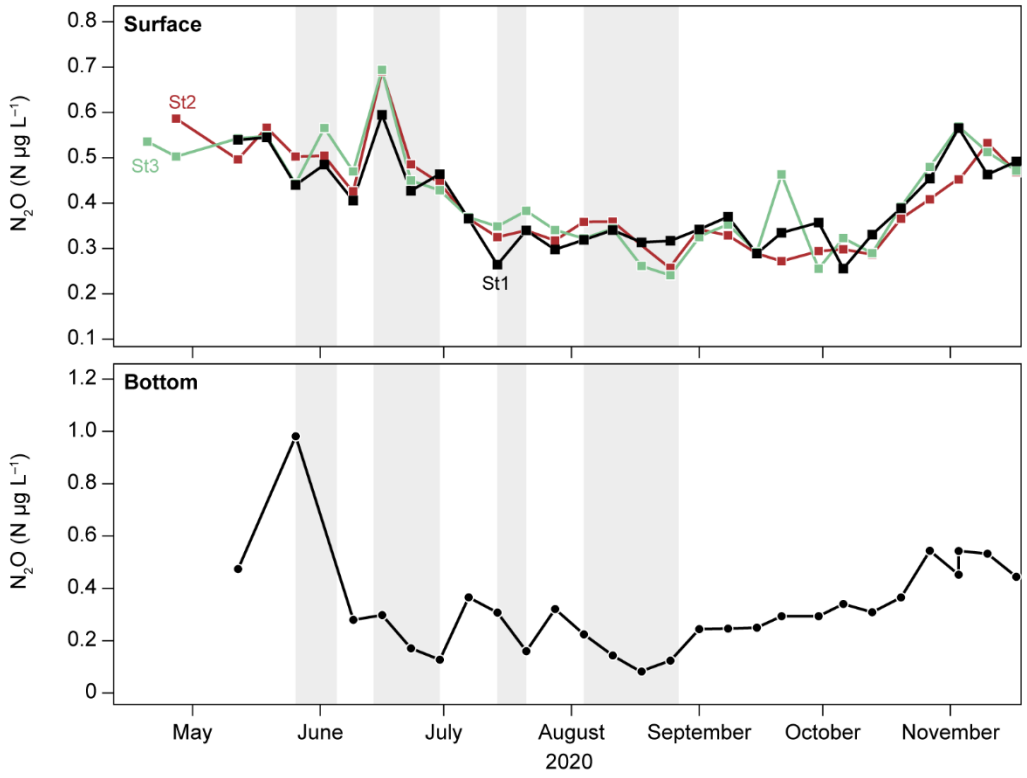

Figure 5 Dissolved N_2O gas concentrations surface and bottom thermal stratification periods highlighted in grey; white background indicate mixed waters

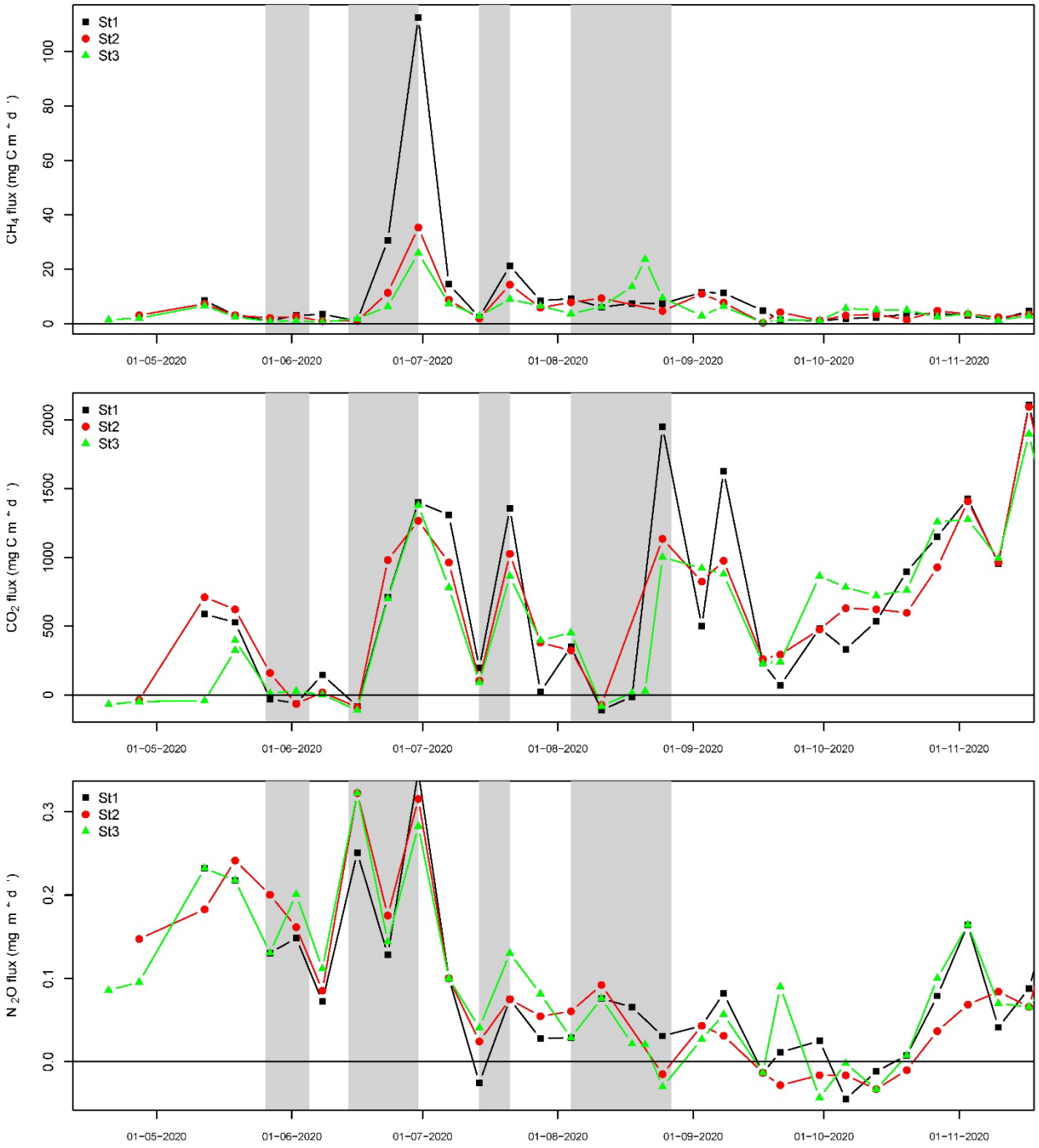

Figure 6. Omstrup lakesurface fluxes of the CH_4, CO_2 and N_2O gases based on dissolved conentration , thermal stratification periods highlighted in grey; white background indicate mixed waters

564

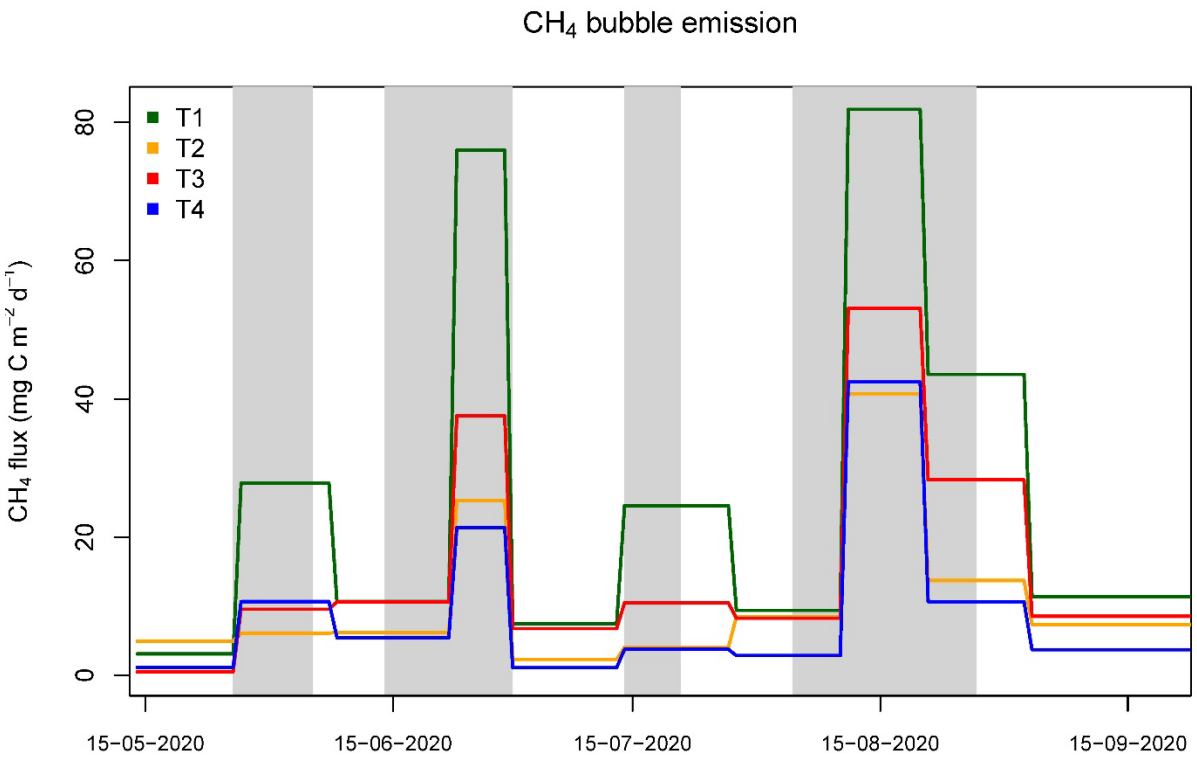

565

566 Figure 7. Plot of CH_4 ebullition averaged for each transect (10 chambers per transect), data collected from
567 40 traps every two weeks. thermal stratification periods highlighted in grey; whitle background indicate
568 mixed waters.

569

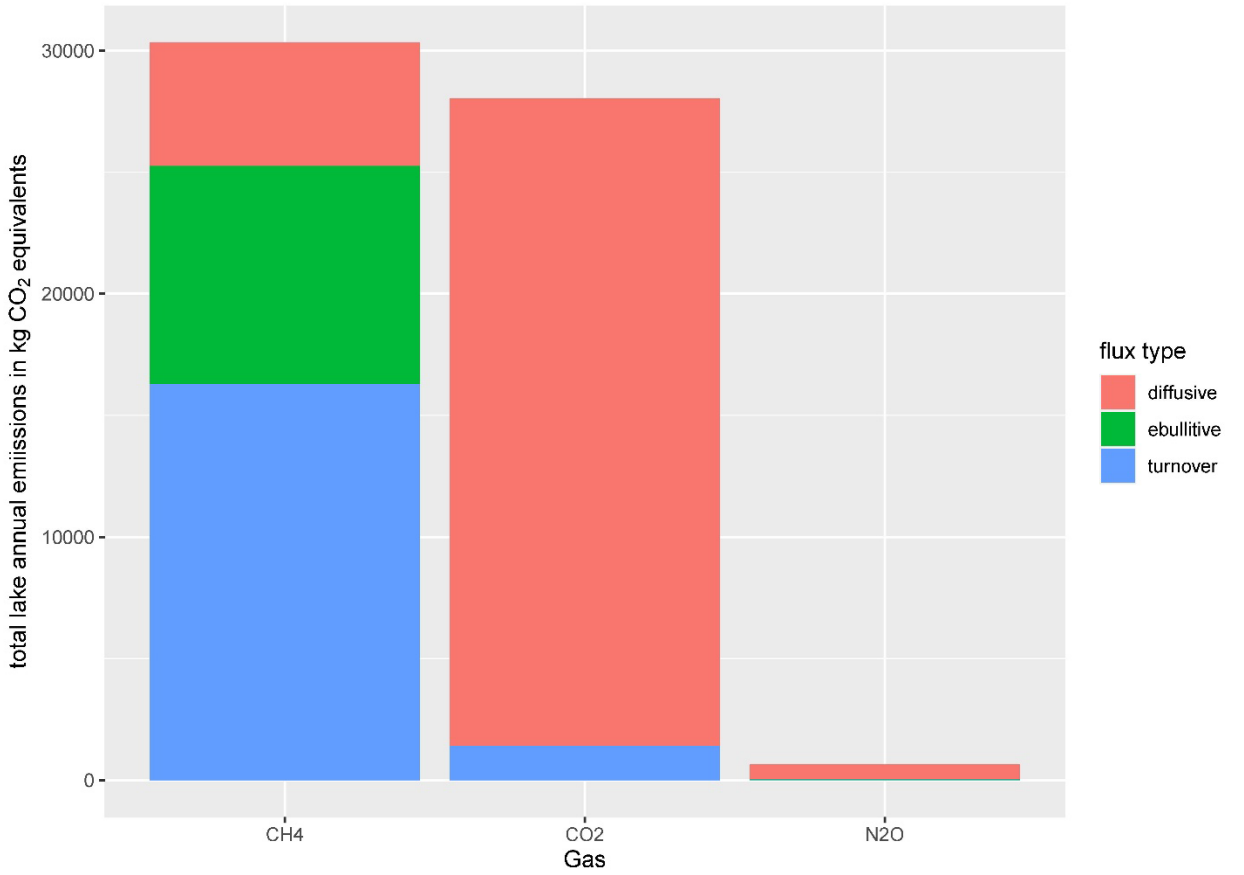

570

571 Figure 8 – Total lake emissions per gas over the growing seasson in CO_2 equivalents. The emissions are
572 divided different emission pathways: Diffusive, ebullitive and turnover flux.

573

574

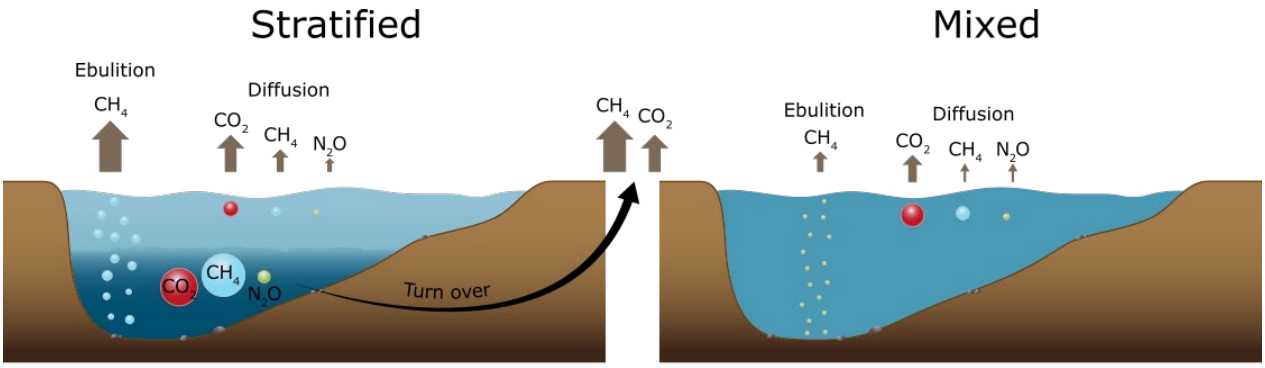

575

576 Figure 9 Summary of different flux types (bubble, diffusive and turnover) for the main greenhouse gases
577 (CH_4 CO_2 and N_2O) observed between the stratified and mixed phases at Ormstrup lake patterns in the
578 stratified and mixed phase. The turnover flux of CH_4 and CO_2 is also represented. The size of the arrow

579 represents the relative amount of emission and the size of the circle in the lake represents the
580 concentration of dissolved gases in stratified or mixed water column.
581

582

References

Aben, R. C. H., Barros, N., van Donk, E., Frenken, T., Hilt, S., Kazanjian, G., Lamers, L. P. M., Peeters, E. T. H. M., Roelofs, J. G. M., de Senerpont Domis, L. N., Stephan, S., Velthuis, M., Van de Waal, D. B., Wik, M., Thornton, B. F., Wilkinson, J., DelSontro, T., and Kosten, S.: Cross continental increase in methane ebullition under climate change, Nat. Comms., 8, 1682, https://doi.org/10.1038/s41467-017-01535-y, 2017.

Audet, J., Carstensen, M. V., Hoffmann, C. C., Lavaux, L., Thiemer, K., and Davidson, T. A.: Greenhouse gas emissions from urban ponds in Denmark, Inland Waters, 1-13, https://doi.org/10.1080/20442041.2020.1730680, 2020.

Bartosiewicz, M., Laurion, I., and MacIntyre, S.: Greenhouse gas emission and storage in a small shallow lake, Hydrobiologia, 757, 101-115, https://doi.org/10.1007/s10750-015-2240-2, 2015.

Bartosiewicz, M., Laurion, I., Clayer, F., and Maranger, R.: Heat-Wave Effects on Oxygen, Nutrients, and Phytoplankton Can Alter Global Warming Potential of Gases Emitted from a Small Shallow Lake, Environ. Sci. Technol., 50, 6267-6275, https://pubs.acs.org/doi/10.1021/acs.est.5b06312, 2016.

Bartosiewicz, M., Przytulska, A., Lapierre, J.-F., Laurion, I., Lehmann, M. F., and Maranger, R.: Hot tops, cold bottoms: Synergistic climate warming and shielding effects increase carbon burial in lakes, Limnol. Oceanogr. Lett., 4, 132-144, https://doi.org/10.1002/lol2.10117, 2019.

Bastviken, D., Cole, J. J., Pace, M. L., and Van de Bogert, M. C.: Fates of methane from different lake habitats: Connecting whole-lake budgets and CH4 emissions, J. Geophys. Res., 113, G02024, https://doi.org/10.1029/2007JG000608, 2008.

Bastviken, D., Nygren, J., Schenk, J., Parellada Massana, R., and Duc, N. T.: Technical note: Facilitating the use of low-cost methane (CH4) sensors in flux chambers – calibration, data processing, and an open-source make-it-yourself logger, Biogeosciences, 17, 3659-3667, https://doi.org/10.5194/bg-17-3659-2020, 2020.

Bastviken, D., Sundgren, I., Natchimuthu, S., Reyier, H., and Gålfalk, M.: Technical Note: Cost-efficient approaches to measure carbon dioxide fluxes and concentrations in terrestrial and aquatic environments using mini loggers, Biogeosciences, 12, 3849-3859, https://doi.org/10.5194/bg-12-3849-2015, 2015.

Bastviken, D., Treat, C. C., Pangala, S. R., Gauci, V., Enrich-Prast, A., Karlson, M., Gålfalk, M., Romano, M. B., and Sawakuchi, H. O.: The importance of plants for methane emission at the ecosystem scale, Aquat. Bot., 184, 103596, https://doi.org/10.1016/j.aquabot.2022.103596, 2023.

Beaulieu, J. J., DelSontro, T., and Downing, J. A.: Eutrophication will increase methane emissions from lakes and impoundments during the 21st century, Nat. Comms., 10, 1-5, https://doi.org/10.1038/s41467-019-09100-5, 2019.

Bergen, T. J. H. M., Barros, N., Mendonça, R., Aben, R. C. H., Althuizen, I. H. J., Huszar, V., Lamers, L. P. M., Lürling, M., Roland, F., and Kosten, S.: Seasonal and diel variation in greenhouse gas emissions from an urban pond and its major drivers, Limnol. Oceanogr., 64, 2129-2139, https://doi.org/10.1002/lno.11173, 2019.

Blees, J., Niemann, H., Wenk, C. B., Zopfi, J., Schubert, C. J., Kirf, M. K., Veronesi, M. L., Hitz, C., and Lehmann, M. F.: Micro-aerobic bacterial methane oxidation in the chemocline and anoxic water column of deep south-Alpine Lake Lugano (Switzerland), Limnol. Oceanogr., 59, 311-324, https://doi.org/10.4319/lo.2014.59.2.0311, 2014.

Cole, J.: Freshwater in flux, Nat. Geosci., 6, 13-14, https://doi.org/10.1038/ngeo1696, 2013.

Cole, J. J. and Caraco, N. F.: Atmospheric exchange of carbon dioxide in a low-wind oligotrophic lake measured by the addition of SF6, Limnol. Oceanogr., 43, 647-656, https://doi.org/10.4319/lo.1998.43.4.0647, 1998.

Davidson, T. A., Audet, J., Jeppesen, E., Landkildehus, F., Lauridsen, T. L., Søndergaard, M., and Syvaranta, J.: Synergy between nutrients and warming enhances methane ebullition from experimental lakes, Nat. Clim. Chang., 8, 156-160, https://doi.org/10.1038/s41558-017-0063-z, 2018.
Davidson, T. A., Audet, J., Svenning, J.-C. C., Lauridsen, T. L., Søndergaard, M., Landkildehus, F., Larsen, S. E., and Jeppesen, E.: Eutrophication effects on greenhouse gas fluxes from shallow-lake mesocosms override those of climate warming, Glob. Chang. Biol., 21, 4449-4463, https://doi.org/10.1111/gcb.13062, 2015.
Deacon, E. L.: Sea-air gas transfer: The wind speed dependence, Bound.- Layer. Meteorol., 21, 31-37, https://doi.org/10.1007/bf00119365, 1981.
Deemer, B. R. and Holgerson, M. A.: Drivers of Methane Flux Differ Between Lakes and Reservoirs, Complicating Global Upscaling Efforts, J. Geophys. Res. Biogeosci. . 126, e2019JG005600, https://doi.org/10.1029/2019JG005600, 2021.
DelSontro, T., Boutet, L., St-Pierre, A., del Giorgio, P. A., and Prairie, Y. T.: Methane ebullition and diffusion from northern ponds and lakes regulated by the interaction between temperature and system productivity, Limnol. Oceanogr., 61, S62-S77, http://doi.wiley.com/10.1002/lno.10335, 2016.
Duc, N. T., Silverstein, S., Lundmark, L., Reyier, H., Crill, P., and Bastviken, D.: Automated flux chamber for investigating gas flux at water–air interfaces, Environ. Sci. Technol., 47, 968-975, 2013.
Erkkilä, K. M., Ojala, A., Bastviken, D., Biermann, T., Heiskanen, J. J., Lindroth, A., Peltola, O., Rantakari, M., Vesala, T., and Mammarella, I.: Methane and carbon dioxide fluxes over a lake: comparison between eddy covariance, floating chambers and boundary layer method, Biogeosciences, 15, 429-445, 10.5194/bg-15-429-2018, 2018.
Esposito, C., Nijman, T. P. A., Veraart, A. J., Audet, J., Levi, E. E., Lauridsen, T. L., and Davidson, T. A.: Activity and abundance of methane-oxidizing bacteria on plants in experimental lakes subjected to different nutrient and warming treatments, Aquat. Bot., 185, 103610, https://doi.org/10.1016/j.aquabot.2022.103610, 2023.
Holgerson, M. A., Richardson, D. C., Roith, J., Bortolotti, L. E., Finlay, K., Hornbach, D. J., Gurung, K., Ness, A., Andersen, M. R., Bansal, S., Finlay, J. C., Cianci-Gaskill, J. A., Hahn, S., Janke, B. D., McDonald, C., Mesman, J. P., North, R. L., Roberts, C. O., Sweetman, J. N., and Webb, J. R.: Classifying Mixing Regimes in Ponds and Shallow Lakes, Water Resour. Res., 58, e2022WR032522, https://doi.org/10.1029/2022WR032522, 2022.
Jespersen, A. and Christoffersen, K.: Measurements of Chlorophyll a from phytoplankton using ethanol as extraction solvent., Archiv für Hydrobiologie, 109, 445-454, 1987.
Kirillin, G. and Shatwell, T.: Generalized scaling of seasonal thermal stratification in lakes, Earth Sci. Rev., 161, 179-190, https://doi.org/10.1016/j.earscirev.2016.08.008, 2016.
Koschorreck, M., Prairie, Y. T., Kim, J., and Marcé, R.: Technical note: CO2 is not like CH4 – limits of and corrections to the headspace method to analyse pCO2 in fresh water, Biogeosciences, 18, 1619-1627, 10.5194/bg-18-1619-2021, 2021.
McAuliffe, C.: Gas chromatographic determination of solutes by multiple phase equilibrium, Chem Technol, 1, 46-51, 1971.
Meerhoff, M., Audet, J., Davidson, T. A., De Meester, L., Hilt, S., Kosten, S., Liu, Z., Mazzeo, N., Paerl, H., Scheffer, M., and Jeppesen, E.: Feedbacks between climate change and eutrophication: revisiting the allied attack concept and how to strike back, Inland Waters, 1-42, https://doi.org/10.1080/20442041.2022.2029317, 2022.
Peacock, M., Audet, J., Jordan, S., Smeds, J., and Wallin, M. B.: Greenhouse gas emissions from urban ponds are driven by nutrient status and hydrology, Ecosphere, 10, e02643, https://doi.org/10.1002/ecs2.2643, 2019.
Peacock, M., Audet, J., Bastviken, D., Cook, S., Evans, C. D., Grinham, A., Holgerson, M. A., Högbom, L., Pickard, A. E., Zieliński, P., and Futter, M. N.: Small artificial waterbodies are widespread and persistent

emitters of methane and carbon dioxide, Glob. Chang. Biol., 27, 5109-5123, https://doi.org/10.1111/gcb.15762, 2021.
Petersen, S. O., Hoffmann, C. C., Schäfer, C. M., Blicher-Mathiesen, G., Elsgaard, L., Kristensen, K., Larsen, S. E., Torp, S. B., and Greve, M. H.: Annual emissions of CH4 and N2O, and ecosystem respiration, from eight organic soils in Western Denmark managed by agriculture, Biogeosciences, 9, 403-422, https://doi.org/10.5194/bg-9-403-2012, 2012.
Pinheiro, J., Bates, D., DebRoy, S., Sarkar, D., and R Core Team: nlme: Linear and Nonlinear Mixed Effects Models, 2014.
R Development Core Team: R: a language and environment for statistical computing. R Foundation for Statistical Computing (4.2.1) [code], 2022.
Rosentreter, J. A., Borges, A. V., Deemer, B. R., Holgerson, M. A., Liu, S., Song, C., Melack, J., Raymond, P. A., Duarte, C. M., Allen, G. H., Olefeldt, D., Poulter, B., Battin, T. I., and Eyre, B. D.: Half of global methane emissions come from highly variable aquatic ecosystem sources, Nat. Geosci., 14, 225-230, https://doi.org/10.1038/s41561-021-00715-2, 2021.
Saarela, T., Rissanen, A. J., Ojala, A., Pumpanen, J., Aalto, S. L., Tiirola, M., Vesala, T., and Jäntti, H.: CH4 oxidation in a boreal lake during the development of hypolimnetic hypoxia, Aquat. Sci., 82, 19, https://doi.org/10.1007/s00027-019-0690-8, 2019.
Schubert, C. J., Diem, T., and Eugster, W.: Methane Emissions from a Small Wind Shielded Lake Determined by Eddy Covariance, Flux Chambers, Anchored Funnels, and Boundary Model Calculations: A Comparison, Environ. Sci. Technol., 46, 4515-4522, https://doi.org/10.1021/es203465x, 2012.
Sø, J. S., Sand-Jensen, K., Martinsen, K. T., Polauke, E., Kjær, J. E., Reitzel, K., and Kragh, T.: Methane and carbon dioxide fluxes at high spatiotemporal resolution from a small temperate lake, Sci. Total Environ., 878, 162895, https://doi.org/10.1016/j.scitotenv.2023.162895, 2023.
Søndergaard, M., Jeppesen, E., Peder Jensen, J., and Lildal Amsinck, S.: Water Framework Directive: ecological classification of Danish lakes, J. Appl. Ecol., 42, 616-629, https://doi.org/10.1111/j.1365-2664.2005.01040.x, 2005.
Søndergaard, M., Nielsen, A., Skov, C., Baktoft, H., Reitzel, K., Kragh, T., and Davidson, T. A.: Temporarily and frequently occurring summer stratification and its effects on nutrient dynamics, greenhouse gas emission and fish habitat use: case study from Lake Ormstrup (Denmark), Hydrobiologia, 850, 65-79, https://doi.org/10.1007/s10750-022-05039-9, 2023.
Thottathil, S. D., Reis, P. C. J., and Prairie, Y. T.: Methane oxidation kinetics in northern freshwater lakes, Biogeochemistry, 143, 105-116, 10.1007/s10533-019-00552-x, 2019.
Wanninkhof, R.: Relationship between wind-speed and gas-exchange over the ocean, J. Geophys. Res. Oceans, 97, 7373-7382, https://doi.org/10.1029/92jc00188, 1992.
Weiss, R. F.: Carbon dioxide in water and seawater: the solubility of a non-ideal gas, Mar. Chem., 2, 203-215, https://doi.org/10.1016/0304-4203(74)90015-2, 1974.
Weiss, R. F. and Price, B. A.: Nitrous oxide solubility in water and seawater, Mar. Chem., 8, 347-359, https://doi.org/10.1016/0304-4203(80)90024-9, 1980.
West, W. E., Coloso, J. J., and Jones, S. E.: Effects of algal and terrestrial carbon on methane production rates and methanogen community structure in a temperate lake sediment, Freshw. Biol., 57, 949-955, https://doi.org/10.1111/j.1365-2427.2012.02755.x, 2012.
Wiesenburg, D. A. and Guinasso, N. L.: Equilibrium solubilities of methane, carbon monoxide, and hydrogen in water and sea water, J. Chem. Eng. Data . 24, 356-360, https://doi.org/10.1021/je60083a006, 1979.
Wik, M., Crill, P. M., Varner, R. K., and Bastviken, D.: Multiyear measurements of ebullitive methane flux from three subarctic lakes, J. Geophys. Res. Biogeosci. . 118, 1307–1321, https://doi.org/10.1002/jgrg.20103, 2013.

Woolway, R. I. and Merchant, C. J.: Worldwide alteration of lake mixing regimes in response to climate change, Nat. Geosci., 12, 271-276, https://doi.org/10.1038/s41561-019-0322-x, 2019.
Yvon-Durocher, G., Allen, A. P., Montoya, J. M., Trimmer, M., and Woodward, G.: The temperature dependence of the carbon cycle in aquatic ecosystems, Adv. Ecol. Res., 43, 267-313, https://doi.org/10.1016/B978-0-12-385005-8.00007-1, 2010.
Yvon-Durocher, G., Allen, A. P., Bastviken, D., Conrad, R., Gudasz, C., St-Pierre, A., Thanh-Duc, N., and del Giorgio, P. A.: Methane fluxes show consistent temperature dependence across microbial to ecosystem scales, Nature, 507, 488-491, https://doi.org/10.1038/nature13164, 2014.
Zhou, Y., Zhou, L., Zhang, Y., de Souza, J. G., Podgorski, D. C., Spencer, R. G. M., Jeppesen, E., and Davidson, T. A.: Autochthonous dissolved organic matter potentially fuels methane ebullition from experimental lakes, Water Res., 166, 115048, https://doi.org/10.1016/j.watres.2019.115048, 2019.